Changes in stream food web structure across a gradient of acid mine drainage increases local community stability

Justin PF Pomeranz[1,*], Jeff S Wesner[2], Jon S Harding[1]

[1]School of Biological Sciences, University of Canterbury, Christchurch, New Zealand

[2]Department of Biology, University of South Dakota, Vermillion, South Dakota

[*]Corresponding Author: jfpomeranz@gmail.com

Running head: AMD food web stability

Abstract

Understanding what makes food webs stable has long been a goal of ecologists. Topological structure and the distribution and magnitude of interaction strengths in food webs have been shown to confer important stabilizing properties. However, our understanding of how variable species interactions affect food web structure and stability is still in its infancy. Anthropogenic stress, such as acid mine drainage, is likely to place severe limitations on the food web structures possible due to changes in community composition and body mass distributions. Here, we used mechanistic models to infer food web structure and quantify stability in streams across a gradient of acid mine drainage. Multiple food webs were iterated for each community based on species pairwise interaction probabilities, in order to incorporate the variability of realistic food web structure. We found that food web structure was altered systematically with a 32-fold decrease in the number of links and a 2-fold increase in connectance across the gradient. Stability generally increased 6-fold with increasing acid mine drainage stress, regardless of how interaction strengths were estimated. However, the distribution of the stability measure, *s*, for some impacted communities separated into clusters of higher and lower magnitude depending on how interaction strengths were estimated. Management and restoration of impacted sites needs to consider their increased stability, as this may have important implications for the re-colonization of desirable species. Furthermore, active species introductions may be required to overcome the internal ecological inertia of affected communities.

Keywords

Interaction probability, traits, anthropogenic impacts, community stability, food webs, streams

Introduction

While research in the last four decades has significantly improved our understanding of food web stability, nearly all of the previous work assumes that network structure is static. Food webs, however, are dynamic. Pairwise species links are variable, and can change through space and time based on resource availability, indirect interactions, and abiotic conditions (Thompson and Townsend 1999, Poisot et al. 2012, Poisot et al. 2015, Poisot et al. 2016). In fact, this variability in trophic interactions has been theorized as promoting stability because consumers will allocate foraging effort differentially based on resource availability, potentially dampening environmental effects on population densities (Kondoh 2003). Likewise, larger predators are generally more mobile and can rapidly moderate their behavior in response to changing resource conditions, which can connect spatially-distant food webs and increase stability across the meta-webs (McCann et al. 2005).

Body size has been shown to be a strong organizing factor in food webs, particularly in aquatic habitats (Cohen et al. 2003, Brose et al. 2006a, Petchey et al. 2008). Body size can determine who interacts with whom, as well as the strength of those interactions. Predators are generally larger than their prey (Brose et al. 2006a) and diet breadth also correlates with body size, resulting in the largest-sized predators consuming the greatest variety of prey body sizes (Brose et al. 2017). Interaction strengths also correlate with predator: prey body size ratios (Emmerson and Raffaelli 2004, Berlow et al. 2009) and these allometries contribute to local food-web stability (Brose et al. 2006b, Tang et al. 2014). Finally, a strong, negative correlation between the positive and negative interaction magnitudes (e.g., effect of resource on consumer, and consumer on resource, respectively) has also been shown to drive stability in natural food webs (Tang et al. 2014).

One global stressor in freshwater ecosystems that may affect food web stability is Acid mine drainage (AMD). Acid mine drainage is often the result of mining activities in geologic strata with high sulfur content and affects stream habitats globally. AMD significantly impacts abiotic conditions with severely lowered pH (e.g., < 3) and high concentrations of dissolved trace metals (e.g., > 20 mg/l; Hogsden and Harding 2012b). AMD is known to decrease community diversity by removing sensitive taxa (Hogsden and Harding 2012b), alter size spectra (Pomeranz et al. 2019b) and simplify food web structure (Hogsden and Harding 2012a). The restoration of AMD-impacted streams remains an important goal for ecologists. However, to our knowledge, no studies of local community stability in AMD-impacted streams currently exist.

Incorporating the variability in species interactions and network structure is an important next frontier in our understanding of food web stability. To determine how variation in species interactions and food web structure affects stability, we used mechanistic models to infer species pairwise interaction probabilities (see below) across a gradient of AMD stress. Here, we solely focus on predator-prey interactions and non-trophic interactions are not included in our analyses (i.e., non-trophic interactions are coded as zeros in the adjacency matrices, see below).

Variability of possible food web topologies was incorporated by conducting multiple Bernoulli trials based on these probabilities, resulting in a distribution of response variables. We used a dataset of stream communities across an AMD stress gradient. AMD stress is known to reduce species richness (Hogsden & Harding, 2012a b), and alter local population densities, and biomass distributions (Pomeranz et al. 2019b). We expected food webs to become simpler (e.g., fewer links), and more connected (e.g., high proportion of potential links realized) with increasing AMD impact. Furthermore, we expected these structural changes to lead to food webs with higher stability.

Methods

Study site and stream characteristics

This study uses data originally published in Pomeranz et al. (2019b). Twenty five streams were sampled in the Buller-Grey region in the north-west of the South Island, New Zealand. The region has spatially-consistent climatic conditions, geology, and freshwater biota (Harding et al. 1997, Harding and Winterbourn 1997), and has a history of coal mining. Thirteen of the streams sampled were known to be affected by AMD (which we refer to as "impacted" streams), there is no urbanization, farming or other significant land use activity in any of these catchments. To our knowledge, the other twelve streams were not affected by AMD inputs, and represented a natural gradient of pH (~ 4 – 7) and low metal concentrations. Although these un-impacted streams represent a wide range of pH values, these occur naturally due to the presence of leaching organic acids from the soil and decomposing vegetation (Hogsden and Harding 2012a, Collier et al. 2016). Furthermore, Collier et al. (1990) have shown that the native aquatic fauna is well-adapted to these conditions, with many of the most widespread insect taxa occurring in streams with a natural pH of 4.5-5. These were sampled in order to capture the range of natural variation present.

Water chemistry variables including pH, and conductivity were measured in the field using standard meters (YSI 550A and YSI 63, YSI Environmental Incorporated, Ohio, USA) and filtered (0.45 μm mixed cellulose ester filter) water samples were analyzed for dissolved metal concentrations (Appendix S1) from all 25 streams. These variables were analyzed using principal components to generate an AMD gradient (Appendix S1: Table S1, Figure S1; Pomeranz et al. 2019b). Principal component (PC) axis 1 explained 78% of the variation among sites, and was strongly correlated with pH and dissolved metal concentrations. Site scores for PC axis 1 were extracted and used as a proxy for the AMD gradient. Un-impacted sites have PC axis 1 scores from -3.6 to ~-0.8. Sites with PC axis 1 values > -0.8 are impacted by AMD, with increasing PC1 values indicating increasing levels of AMD stress.

Community sampling and body mass estimation

Benthic macroinvertebrates were randomly collected in three Surber samples (0.06 m^2, 0.25 mm mesh) from riffle and run habitats at each site (Blakely and Harding, 2005). Individuals were identified to the lowest practical taxonomic level and the body mass (dry weight) of all individuals were estimated based on taxon-specific length-weight regressions (Towers et al. 1994, Stoffels et al. 2003). Linear measurements of all individuals were measured according to the methods of Towers et al. (1994) and Stoffels et al. (2003). Body mass estimates were averaged by taxa for each site where they occurred.

Fish were sampled using quantitative electrofishing techniques from a 20 m reach within each site (Hogsden and Harding 2012a). Stop nets were placed at the top and bottom of the reach and fish were removed during three successive passes (Bertrand et al. 2006, Reid et al. 2009). Fish population densities were estimated using the k-pass removal method of Seber and Le Cren (1967). All fish captured had their lengths measured and were converted to dry weight estimates using length-weight regressions for New Zealand fish (Jellyman et al. 2013). Mean dry weight estimates for each fish taxa were calculated as above.

Previous analyses of this data set have shown that increasing AMD-stress has altered community structure consistently. Fish were completely absent in AMD impacted streams, and most large-bodied invertebrate predators were also removed (Pomeranz et al. 2019b). Un-impacted communities were dominated by mayflies, stoneflies, and caddisflies. Communities across the AMD gradient were dominated by aquatic worms (Oligachaete) and true-flies, predominantly the families Chironomidae and Empididae. Although previous work on AMD-impacted streams in this region of New Zealand have shown declines in species richness (Hogsden & Harding, 2012a), explicit analyses of species richness in the dataset presented in Pomeranz *et al.*, (2019b) were not previously conducted. Therefore, we analyzed how species richness responds to AMD-stress here (see Bayesian analyses below)

Inferring food-web structure

To estimate food web structure at each of the 25 sites, we used a mechanistic model that estimates the probability of pairwise species interactions based on niche and neutral processes (Figure 1; Bartomeus et al. 2016, Pomeranz et al. 2019a). To achieve this, we used the `Traitmatch` package (Bartomeus et al. 2016) in the R statistical language (R Development Core Team, 2017) to infer niche processes (Appendix S2). Specifically, we used empirical predator-prey body sizes from Broadstone Stream and Tadnoll Brook, (Woodward et al. 2010) to estimate the probability that species would interact based on their body sizes. The parameterized `Traitmatch` model correctly assigned high probabilities (> 0.7) to 57% of the realized interactions in the data from Broadstone Stream and Tadnoll Brook, indicating adequate fit. Only 25% of the realized interactions received probabilities < 0.5. After parameterizing the model, we inferred the probability of all pairwise interactions at each site based on local species average body sizes. Species interaction probability vectors were converted to square (S x S, where S = the number of taxa present) interaction probability matrices, **P** (Figure 1A)**.** Columns and rows of **P** represent species in their role as consumers and resources, respectively. Therefore, $\mathbf{P}_{ij}$ represents the probability that species j consumes species i. The matrices were ordered by increasing body size from left to right, and top to bottom.

After inferring the probabilities of all possible pairwise interactions, we further refined these possible interactions by restricting niche forbidden links (*sensu* Morales-Castilla et al. 2015, Pomeranz et al. 2019a). Niche forbidden links were defined as in Pomeranz et al. (2019a). We restricted predatory interactions between animals which are known to be non-predatory, or which lacked morphological adaptations for the consumption of animal prey (e.g., set $P_{\bullet j}$ to 0, Appendix S2: Figure S2). For example, members of the mayfly genus, *Deleatidium*, have mouthparts modified for "brushing" diatoms off benthic surfaces, and lack the ability to consume animal prey. Conversely, net-spinning caddisflies in the family Hydropsychidae construct nets to filter feed, but retain chewing mouthparts and are able to consume animal prey they capture, so their predation probabilities were not modified. These designations were based on morphology as opposed to traditional functional feeding group classifications, in order to prune predatory interactions conservatively. Niche forbidden taxa in this study are presented in Appendix S2: Table S1.

To account for neutral effects (*sensu* Canard et al. 2014) we scaled these probability estimates based on local relative abundances. This simply takes into account that two rare species are less likely to interact than two abundant species. The modified interaction probabilities for each site were calculated as $\mathbf{P}_{ij}' = \mathbf{P}_{ij} * \mathbf{N}_{ij}$, where $\mathbf{N}_{ij}$ is the product of relative abundances of species *i* and *j*, scaled from 0.5 to 1 respectively (Figure 1A-C). Abundant species pairs = 1 and are assumed to interact based on niche probabilities, while rare species pairs = 0.5 and are less likely to encounter one another, so their overall interaction probabilities are reduced (see Appendix S2 for a discussion on selection of scaled values). The modified probabilities in $\mathbf{P}_{ij}'$ were rescaled from 0.01 to 0.99 (Figure 1D) in order to put them on a meaningful scale for inferring adjacency matrices (see below).

Finally, the probability matrices for each stream were converted to 250 binary adjacency matrices **A** (Figure 1E). We chose 250 trials because this generally captured all observed interactions in an empirical stream food web from New Zealand without over predicting the number of links (Appendix S2: Fig. S7). Adjacency matrices are square matrices with taxa in their role as predators in columns and their role as prey in rows as in the probability matrices (**P**), where $\mathbf{A}_{ij} = 1$ when taxa *j* consumes taxa *i*, and 0 otherwise. This was done by conducting Bernoulli (i.e. binomial) trials, where the probability that $\mathbf{A}_{ij} = 1 = \mathbf{P'}_{ij}$. This allowed us to assess the effect of variable food-web structure on network measurements and stability (see below).

Food-web measures

We calculated a suite of standard food-web measures including the number of links (L), connectance ($C = L / S^2$, where S = the number of species), normalized vulnerability (mean number of consumer species per resource species) and normalized generality (mean number of resource species per consumer species) for all 6250 Adjacency matrices (25 sites x 250 Bernoulli trials). Vulnerability and generality for each iteration were normalized to the size of the food web by dividing by S which makes the measures comparable across networks of different size (Williams and Martinez 2000).

Interaction strength

The adjacency matrices $\mathbf{A}_{ij}$ calculated above, were transformed into Jacobian matrices, where the element $\mathbf{J}_{ij}$ quantifies the effect that species *j* has on species *i* growth rate. For antagonistic (e.g., predatory) interactions assessed here, $\mathbf{J}_{ij} > 0$ (positive effect of resource on consumer) and $\mathbf{J}_{ji} < 0$ (negative effect of consumer on resource). The magnitude, distribution, and correlation of interaction strengths are known to be an important component of food-web stability (Tang et al. 2014). In order to assess the effects of network structure (presence/absence of links), and the effects of interaction strength distributions and correlations, we estimated interaction strengths in four ways: 1) Random interaction strength to test the effects of network topology. Using the methods of Sauve et al. (2016), we estimated all non-zero elements of **J** by sampling them from a half normal distribution $|(\mu = 1, \sigma^2 = 0.1)|$ and multiplied the positive and negative interactions by 1 and -1, respectively; 2) Scaling interaction strengths by body size. Interaction strength is known to scale with predator: prey body size ratios, and this has been suggested as a key process increasing stability in natural food webs (Brose et al. 2006b). To examine these effects, we again sampled interaction strengths from a half normal distribution, but scaled them by predator:prey body size ratios (e.g., smallest positive and greatest negative effects between large predators and small prey); 3) Correlating the top-down (negative effect of predator on prey) and bottom-up (positive effect of prey on predator) interaction strengths. The correlation between positive and negative interactions has been shown to have important implications in local stability (Tang et al. 2014), with the magnitude of negative effects being greater than the magnitude of positive effects. For this, we sampled the negative interactions from a half normal distribution, and correlated the corresponding positive interactions by a factor of 0.7 correlated (e.g., positive interactions = 0.7 × negative interactions). This can be interpreted as a 70% conversion efficiency of prey biomass by predators from stream habitats as estimated from empirical studies (Woodward et al. 2005, Montoya et al. 2009). 4) Interaction strengths scaled by body size and positive and negative interactions correlated. Here, we sampled the negative effects as in (3), and scaled them by predator:prey body size ratios. We then calculated the corresponding positive effects by multiplying the scaled negative effect by 0.7. This takes into account the scaling of interaction strengths by body size and the correlation of positive and negative effects. For all interaction strength estimates, we used a modified version of the `jacobian_binary()` function available in the supplemental information from Sauve et al. (2016)

Stability

For each adjacency matrix (25 streams × 250 trials = 6,250 matrices), interaction strengths were estimated in one of four ways (see above) and a stability analysis was conducted. Here, a network is defined as stable if all of the real parts of its eigenvalues are negative. The stability metric, s, was defined as the minimum amount of intraspecific competition (e.g., the diagonal of the Jacobian matrix, $\mathbf{J}_{ii}$) necessary for a food-web iteration to be stable (Neutel et al. 2002, Tang et al. 2014, Sauve et al. 2016). Smaller values of s are considered to be more stable (Neutel et al. 2002, Sauve et al. 2016), however, there is no known value or threshold of s which separates networks from being stable or not. Lower values of s simply imply that that network is *more* stable than high values of s. We calculated the s metric using the `stability()` function available in the supplementary information of Sauve et al. (2016). Specifically, values on the diagonal of the Jacobian matrices (i.e. intraspecific competition), were varied until the individual matrix was stable (e.g., all of the real parts of the eigenvalues were negative). The same value for intraspecific competition was used for each element of the diagonal (e.g., $\mathbf{J}_{ii} = s$). This method is equivalent to that used by Allesina and Tang, (2012) and Tang et al. (2014) as discussed in Appendix S1 of Sauve et al. (2016).

Bayesian analyses

We tested the relationship between response variables (species richness, food web measures, stability) and the AMD stress gradient using generalized linear mixed models in R (R Development Core Team 2017). All models used a gamma likelihood with a log link and included site identity as a random intercept. We used weakly informative priors for the intercept and slope, both of which were normal with a mean of 0 and a standard deviation of 1 [$N(0,1)$]. The prior for the shape parameter of the gamma distribution was a default prior of gamma(0.01,0.01).

Models were fit using Bayesian inference with posterior distributions generated using Hamiltonian Monte Carlo method in `rstan` (Stan Development Team 2018) via the `brms` package (Bürkner 2018) in R. For each model, we ran four chains each with 2000 iterations, with the first 1000 iterations discarded as warm-up. Convergence was checked by ensuring that all r-hats were < 1.1, and by visually assessing trace plots (Gelman and Rubin 1992). All models achieved convergence. To assess model performance, we used posterior predictive checks in which we simulated ten datasets from the posterior distribution and graphically compared them to the original dataset. Differences between the original and simulated data would indicate structural problems in the model (Gabry et al. 2018). To assess the influence of the prior, we plotted the prior and posterior distributions. All plots indicated little influence of the prior on the posterior (Appendix S3: Figs. S1-9).

All data used in this analysis are available at [Data Dryad DOI here upon article acceptance]. An example dataset and R script to run the methods presented here are available at 10.5281/zenodo.3754676. Annotated R scripts for the full analysis presented here are available from the corresponding author upon request.

Results

Species richness and food-web measures

Total species richness and all food-web measures responded to the AMD gradient (Table 1, Figure 2). Total taxonomic richness declined by 19% (CrI: 14-24%) with each unit increase in PC axis 1 (e.g., increasing AMD stress). For example, reference sites had a median of 7.4 (CrI

4.2-13.8) times as many species compared to sites with high AMD stress. The number of inferred links decreased by a median of 30% (CrI: 22-39%) with each unit increase in PC axis 1 (e.g., increasing AMD stress). For example, reference sites had a median of 2.7 (CrI: 2-3.9) times more links compared to sites with moderate AMD stress, and 32.1 (CrI: 10.7-115.8) times more links compared to the sites with high AMD stress. The median number of links in sites with moderate AMD stress was 12 (CrI: 5.5-30) times that observed in sites with high AMD stress (Table 1). In contrast, the median value for connectance increased by 7% (CrI: 3-11%) across the AMD stress gradient. Likewise, both normalized generality and vulnerability increased by 9% (CrI: 5-13%) and 14% (CrI: 10-19%), respectively.

Stability

Stability increased (lower s indicates higher stability) with increasing AMD stress (Table 2, Figure 3). The value of s decreased by ~ 23% with each unit increase in the AMD stress gradient (Table 2). This finding was consistent across all methods of estimating interaction strengths (i.e. sampling interaction strengths randomly, scaling interaction strengths by body size, correlating positive and negative interaction strengths, and the combination of scaling and correlating interaction strengths). While the response of s across the gradient had the same general shape regardless of how interaction strengths were estimated, there are some key differences between them. First, the range of s when scaling the interaction strengths by body size was lower for all networks than all other interaction strength estimations (Figure 3B). Second, when interaction strengths were correlated (e.g., positive interactions = 0.7 × negative interactions), the distribution of s for some of the impacted streams separates into distinct clusters (Figure 3, lower panel) indicating that impacted sites can have more and less stable structures, whereas the stability of un-impacted food web structures are more evenly distributed.

Discussion

We used mechanistic models to infer the structure and stability of food webs across an acid mine drainage (AMD) stress gradient based on interaction probabilities determined by the local distribution of macroinvertebrate and fish body sizes and population densities. Our results show that AMD impacts lead to small, simple, and stable food webs. Furthermore, this study adds to our understanding of the stabilizing attributes of food webs, including topological structure, distribution of body sizes, and interaction strengths.

Inferred network structure

Species richness declined across the AMD gradient. Likewise, community structure was simplified, namely due to the loss of the largest sized taxa (e.g., fish, large-bodied invertebrates) Pomeranz et al. 2019b). This is consistent with the findings of several studies showing a decline in species richness and trophic levels in response to AMD inputs (reviewed in Hogsden and Harding 2012b). The number of inferred pairwise interactions (e.g., feeding links) also decreased across the AMD gradient. A reduction in links may translate to less energy pathways available (Hogsden and Harding 2013), reducing ecological efficiency or functional diversity (Petchey and Gaston 2002). Likewise, the interaction magnitude in food webs with fewer links may increase relative to webs with many links. Having a few strong links is generally considered to be destabilizing (Wootton and Stouffer 2015). On the other hand, because interaction strengths are related to body size and AMD inputs cause the loss of the largest-sized predators (Pomeranz et al. 2019b), the links present in impacted streams may be weak, possibly increasing stability. Indeed, when interaction strengths were scaled based on body size (see below) the stability metric, s, was lower (i.e. more stable) across all networks when compared to randomly sampled interaction strengths (e.g., scale of y-axis in Fig. 3A and 3B).

Connectance increased across the AMD gradient, which means that a high proportion of the possible links in the food web were realized. This is in agreement with previous work which has shown a negative relationship between network size and connectance (Schmid-Araya et al. 2002). Normalized generality and normalized vulnerability also increased across the AMD gradient, meaning that each resource taxa was exploited by a high proportion of the consumer taxa present, and also that each consumer taxa was exploiting a high proportion of the resource taxa available. These results support findings of previous studies on food webs in AMD impacted streams (Hogsden and Harding 2012a), and indicate a re-organization of food web structure resulting in small, simple, and well-connected communities.

Distribution of interaction strengths

Scaling interaction strengths based on body size increased stability (lower values of s) for all streams across the AMD gradient compared with sampling interaction strengths randomly, which is in agreement with previous studies (Emmerson and Raffaelli 2004, Otto et al. 2007). When positive and negative interaction strengths were correlated, the distribution of the stability metric across all sites was similar to that observed when sampling interaction strengths randomly. However, in some impacted streams, the distribution of the stability metric clustered into two or more distinct magnitudes e.g., an individual stream has configurations which were more or less stable. The configurations that were less stable have stability metric distributions similar to un-impacted streams, potentially making them good candidates for restoration. For example, stable communities generally have high resistance to species introductions, but a typical goal of restoration is often the re-establishment of the pre-disturbance community composition, or the return of sensitive species (Lockwood and Pimm 1999). Therefore, focusing restoration actions on impacted communities that are less stable may provide a higher likelihood of re-colonization by desirable species. Communities which are less stable may have lower biological resistance (*sensu* Frost et al. 2006) or internal ecological inertia (*sensu* Gray et al. 2016) to the re-colonization of previously extirpated sensitive taxa. Indeed, alternations between more and less stable food web configurations has been observed during community succession in soil food webs (Neutel et al. 2007). Stability decreased as the biomass of the top trophic level increased, and stability increased when the addition of a new top predator alleviated predation pressure on the lower trophic levels. Although stability was not directly measured, this is similar to the observed re-organization of food web structure with the re-colonization of successively larger sized predators in Broadstone Stream (Layer et al. 2011, Gray et al. 2014).

Conclusions

Our results indicate that AMD inputs consistently alter food-web structure, and that some AMD-impacted streams may be more receptive to restoration than others. When interaction strengths are estimated with more biologically-relevant values (e.g., scaling and correlating magnitude) some of the impacted streams have stability values similar to un-impacted streams. For successful restoration of all streams, the chemical conditions need to be returned to a pre-disturbance state. Impacted streams which are less stable may lack internal inertia and have low resistance to species invasions and only require chemical remediation to place them on a trajectory of community succession. However, in impacted streams with high food web stability, beneficial disturbances (e.g., scouring flood) or active species reintroductions may need to occur to overcome the internal ecological inertia of these communities. This is because small, stable communities have high resistance to changes in community composition and may inhibit the successful colonization of desirable species. However, because of their lower stability, it may also be necessary to actively monitor the sites to ensure that non-desirable (e.g., exotic invasive) species do not colonize the site.

Further work is needed to understand the effect of species introductions. If the goal of a restoration activity is for community composition to be similar to a pre-disturbance state, or the return of species with commercial value (e.g., fisheries), it may be necessary to set the community on a trajectory of community assembly, rather than introduce the desired species at the outset (i.e. the "myth of fast-forwarding" *sensu* Hilderbrand et al. 2005). For example, it may be necessary to introduce primary or secondary consumers (e.g., grazers, filter-feeders) in order to increase ecological efficiency and make more energy available for the successful establishment of higher trophic levels (Pimm 1982, Thompson and Townsend 2005). Likewise, it may be necessary to introduce medium sized predators (e.g., as occurred naturally in Broadstone Stream, Layer et al. 2011) in order to restructure the food web architecture before larger predators (e.g., fish) can successfully colonize the site.

Acknowledgements

Thanks to Guy Woodward and Iwan Jones for providing individual interaction data, and to Ignasi Bartomeus and Dominique Gravel for providing the `predict.niche.prob()` function in R to predict new interaction probability values. We would also like to thank Carlyn Perovich, Phil Jellyman, and Kristy Hogsden for thoughtful discussions, as well as Tim Poisot and Jon Borelli for discussions of local stability.

Literature Cited

Allesina S. & Tang S. (2012). Stability criteria for complex ecosystems. *Nature* **483**, 205–208. https://doi.org/10.1038/nature10832

Bartomeus I., Gravel D., Tylianakis J.M., Aizen M.A., Dickie I.A. & Bernard-Verdier M. (2016). A common framework for identifying linkage rules across different types of interactions. *Functional Ecology* **30**, 1894–1903. https://doi.org/10.1111/1365-2435.12666

Berlow E.L., Dunne J.A., Martinez N.D., Stark P.B., Williams R.J. & Brose U. (2009). Simple prediction of interaction strengths in complex food webs. *Proceedings of the National Academy of Sciences* **106**, 187–191

Blakely T.J. & Harding J.S. (2005). Longitudinal patterns in benthic communities in an urban stream under restoration. *New Zealand Journal of Marine and Freshwater Research* **39**, 17–28. https://doi.org/10.1080/00288330.2005.9517291

Brose U., Blanchard J.L., Eklöf A., Galiana N., Hartvig M., R. Hirt M., *et al.* (2017). Predicting the consequences of species loss using size-structured biodiversity approaches. *Biological Reviews* **92**, 684–697. https://doi.org/10.1111/brv.12250

Brose U., Jonsson T., Berlow E.L., Warren P., Banasek-Richter C., Bersier L.-F., *et al.* (2006a). Consumer-resource body-size relationships in natural food webs. *Ecology* **87**, 2411–2417. https://doi.org/10.1890/0012-9658(2006)87[2411:CBRINF]2.0.CO;2

Brose U., Williams R.J. & Martinez N.D. (2006b). Allometric scaling enhances stability in complex food webs. *Ecology Letters* **9**, 1228–1236. https://doi.org/10.1111/j.1461-0248.2006.00978.x

Bürkner P.-C. (2018). Advanced Bayesian multilevel modeling with the R package brms. *The R Journal* **10**, 395–411. https://doi.org/10.32614/RJ-2018-017

Canard E., Mouquet N., Mouillot D., Stanko M., Miklisova D. & Gravel D. (2014). Empirical evaluation of neutral interactions in host-parasite networks. *The American Naturalist* **183**, 468–479. https://doi.org/10.1086/675363

Cohen J.E., Jonsson T. & Carpenter S.R. (2003). Ecological community description using the food web, species abundance, and body size. *Proceedings of the National Academy of Sciences* **100**, 1781–1786

Collier K.J., Ball O.J., Graesser A.K., Main M.R., Winterbourn M.J., Collier K.J., *et al.* (2016). Do Organic and Anthropogenic Acidity Have Similar Effects on Aquatic Fauna? **59**, 33–38

Emmerson M.C. & Raffaelli D. (2004). Predator–prey body size, interaction strength and the stability of a real food web. *Journal of Animal Ecology* **73**, 399–409

Frost T.M., Fischer J.M., Klug J.L., Arnott S.E. & Montz P.K. (2006). Trajectories Of Zooplankton Recovery In The Little Rock Lake Whole-Lake Acidification Experiment. *Ecological Applications* **16**, 353–367. https://doi.org/10.1890/04-1800

Gabry J., Simpson D., Vehtari A., Betancourt M. & Gelman A. (2018). Visualization in Bayesian workflow. *Journal of the Royal Statistical Society Series A*

Gelman A. & Rubin D.B. (1992). Inference from iterative simulation using multiple sequences. *Statistical Science* **7**, 457–511

Gray C., Baird D.J., Baumgartner S., Jacob U., Jenkins G.B., O'Gorman E.J., *et al.* (2014). Ecological networks: the missing links in biomonitoring science. *Journal of Applied Ecology* **51**, 1444–1449. https://doi.org/10.1111/1365-2664.12300

Gray C., Hildrew A.G., Lu X., Ma A., Mcelroy D. & Monteith D. (2016). Recovery and nonrecovery of freshwater food webs from the effects of acidification. *Advances in Ecological Research* **55**, 475–534. https://doi.org/10.1016/bs.aecr.2016.08.009

Harding J.S. & Winterbourn M.J. (1997). An ecoregion classification of the South Island, New Zealand. *Journal of environmental management* **51**, 275–287

Harding J.S., Winterbourn M.J. & McDiffett W.F. (1997). Stream faunas and ecoregions of the South Island, New Zealand: do they correspond? *Archiv für Hydrobiologie* **140**, 289–307

Hilderbrand R.H., Watts A.C. & Randle A.M. (2005). The myths of restoration ecology. *Ecology and Society* **10**. https://doi.org/10.5751/ES-01277-100119

Hogsden K.L. & Harding J.S. (2012a). Anthropogenic and natural sources of acidity and metals and their influence on the structure of stream food webs. *Environmental Pollution* **162**, 466–474. https://doi.org/10.1016/j.envpol.2011.10.024

Hogsden K.L. & Harding J.S. (2012b). Consequences of acid mine drainage for the structure and function of benthic stream communities: a review. *Freshwater Science* **31**, 108–120. https://doi.org/10.1899/11-091.1

Hogsden K.L. & Harding J.S. (2013). Leaf breakdown, detrital resources, and food webs in streams affected by mine drainage. *Hydrobiologia* **716**, 59–73. https://doi.org/10.1007/s10750-013-1544-3

Kondoh M. (2003). Foraging adaptation and the relationship between food-web complexity and stability. *Science* **299**, 1388–1391. https://doi.org/10.1126/science.1079154

Layer K., Hildrew A.G., Jenkins G.B., Riede J.O., Stephen J., Townsend C.R., *et al.* (2011). Long-term dynamics of a well-characterised food web: four decades of acidification and recovery in the Broadstone Stream model system. *Advances in Ecological Research* **44**, 69–117. https://doi.org/10.1016/B978-0-12-374794-5.00002-X

Lockwood J.L. & Pimm S.L. (1999). When does restoration succeed? In: *Ecological assembly rules: perspectives, advances and retreats*. (Eds E. Weiher & P.A. Keddy), pp. 363–392. Cambridge University Press, Cambridge, UK.

McCann K.S., Rasmussen J.B. & Umbanhowar J. (2005). The dynamics of spatially coupled food webs. *Ecology Letters* **8**, 513–523. https://doi.org/10.1111/j.1461-0248.2005.00742.x

Montoya J.M., Woodward G., Emmerson M.C. & Solé R.V. (2009). Press perturbations and indirect effects in real food webs. *Ecology* **90**, 2426–2433. https://doi.org/10.1890/08-0657.1

Morales-Castilla I., Matias M.G., Gravel D. & Arau M.B. (2015). Inferring biotic interactions from proxies. *Trends in Ecology & Evolution* **30**, 347–356. https://doi.org/10.1016/j.tree.2015.03.014

Neutel A., Heesterbeek J.A.P., van de Koppel J., Hoenderboom G., Vos A., Kaldeway C., *et al.* (2007). Reconciling complexity with stability in naturally assembling food webs. *Nature* **449**, 599–602. https://doi.org/10.1038/nature06154

Neutel A., Heesterbeek J.A.P. & de Ruiter P.C. (2002). Stability in real food webs: weak links in long loops. *Science* **296**, 1120–1124

Otto S.B., Rall B.C. & Brose U. (2007). Allometric degree distributions facilitate food-web stability. *Nature* **450**, 1226–1229. https://doi.org/10.1038/nature06359

Petchey O.L., Beckerman A.P., Riede J.O. & Warren P.H. (2008). Size, foraging, and food web structure. *Proceedings of the National Academy of Sciences* **105**, 4191–4196

Petchey O.L. & Gaston K.J. (2002). Extinction and the loss of functional diversity. *Proceedings of the Royal Society B* **269**, 1721–1727. https://doi.org/10.1098/rspb.2002.2073

Pimm S.L. (1982). *Food webs*. University of Chicago Press, Chicago.

Poisot T., Canard E., Mouillot D., Mouquet N. & Gravel D. (2012). The dissimilarity of species interaction networks. *Ecology Letters* **15**, 1353–1361. https://doi.org/10.1111/ele.12002

Poisot T., Cirtwill A.R., Cazelles K., Gravel D., Fortin M.-J. & Stouffer D.B. (2016). The structure of probabilistic networks. *Methods in Ecology and Evolution* **7**, 303–312. https://doi.org/10.1111/2041-210X.12468

Poisot T., Stouffer D.B. & Gravel D. (2015). Beyond species: why ecological interaction networks vary through space and time. *Oikos* **124**, 243–251. https://doi.org/10.1111/oik.01719

Pomeranz J.P.F., Thompson R.M., Poisot T. & Harding J.S. (2019a). Inferring predator–prey interactions in food webs. *Methods in Ecology and Evolution* **10**, 356–367. https://doi.org/10.1111/2041-210X.13125

Pomeranz J.P.F., Warburton H.J. & Harding J.S. (2019b). Anthropogenic mining alters macroinvertebrate size spectra in streams. *Freshwater Biology* **64**, 81–92. https://doi.org/10.1111/fwb.13196

Pomeranz J.P.F., Warburton H.J. & Harding J.S. (2018). Anthropogenic mining alters macroinvertebrate size spectra in streams. *Freshwater Biology* **0**. https://doi.org/10.1111/fwb.13196

R Development Core Team (2017). *R: A language and environment for statistical computing*. R Core Team, Vienna, Austria.

Sauve A.M.C., Thébault E., Pocock M.J.O. & Fontaine C. (2016). How plants connect pollination and herbivory networks and their contribution to community stability. *Ecology* **97**, 908–917

Schmid-Araya J.M., Schmid P.E., Robertson A., Winterbottom J., Gjerløv C. & Hildrew A.G. (2002). Connectance in stream food webs. *Journal of Animal Ecology* **71**, 1056–1062. https://doi.org/10.1046/j.1365-2656.2002.00668.x

Seber G.A.F. & Le Cren E.D. (1967). Estimating Population Parameters from Catches Large Relative to the Population. *Journal of Animal Ecology* **36**, 631–643. https://doi.org/10.2307/2818

Stan Development Team (2018). *RStan: the R interface to Stan*.

Stoffels R.J., Karbe S. & Paterson R.A. (2003). Length-mass models for some common New Zealand littoral-benthic macroinvertebrates, with a note on within-taxon variability in parameter values among published models. *New Zealand Journal of Marine and Freshwater Research* **37**, 449–460. https://doi.org/10.1080/00288330.2003.9517179

Tang S., Pawar S. & Allesina S. (2014). Correlation between interaction strengths drives stability in large ecological networks. *Ecology Letters* **17**, 1094–1100. https://doi.org/10.1111/ele.12312

Thompson R.M. & Townsend C.R. (2005). Food-web topology varies with spatial scale in a patchy environment. *Ecology* **86**, 1916–1925

Thompson R.M. & Townsend C.R. (1999). The effect of seasonal variation on the community structure and food-web attributes of two streams: implications for food-web science. *Oikos* **87**, 75–88

Towers D.J., Henderson I.M. & Veltman C.J. (1994). Predicting dry weight of New Zealand aquatic macroinvertebrates from linear dimensions. *New Zealand Journal of Marine and Freshwater Research* **28**, 159–166. https://doi.org/10.1080/00288330.1994.9516604

Williams R.J. & Martinez N.D. (2000). Simple rules yield complex food webs. *Nature* **404**, 180–183. https://doi.org/10.1038/35004572

Woodward G., Ebenman B., Emmerson M., Montoya J.M., Olesen J.M., Valido A., *et al.* (2005). Body size in ecological networks. *Trends in Ecology & Evolution* **7**, 402–409. https://doi.org/10.1016/j.tree.2005.04.005

Wootton K.L. & Stouffer D.B. (2015). Many weak interactions and few strong; food-web feasibility depends on the combination of the strength of species' interactions and their correct arrangement. *Theoretical Ecology* **9**, 185–195. https://doi.org/10.1007/s12080-015-0279-3

Tables

Table 1. Parameter estimates and 95% credible intervals for the effects of the AMD mining gradient on food web measures. Slope estimates < 1 indicate a negative response, and those > 1 indicate positive response (e.g., slope estimate of 0.7 indicates that the value of y decreases by 1-0.7 = 0.3 with every unit increase in the AMD gradient). Shape parameters are excluded from the table. The relative change values were calculated from the posterior distributions of each model. AMD impacts start at ~ -0.8 on PC axis 1, and maximum impacts are represented by values of ~-6 on PC axis 1

	Model				Relative change			
Food Web Measure	Parameter	Median	2.5%	97.5%	Derived quantity	Median	2.5%	97.5%
Species Richness	Intercept	13	11	16	Reference / Moderate AMD	1.77	1.5	2.1
	Slope	0.81	0.76	0.86	Reference / High AMD	7.4	4.2	13.8
					Moderate / High AMD	4.2	2.8	6.5
Links	Intercept	16.4	11.0	24.0	Reference / Moderate AMD	2.7	2.0	3.9
	Slope	0.7	0.6	0.8	Reference / High AMD	32.1	10.7	115.8
					Moderate / High AMD	12.0	5.5	30.0
Connectance	Intercept	0.1	0.1	0.1	Reference / Moderate AMD	0.8	0.8	0.9
	Slope	1.1	1.0	1.1	Reference / High AMD	0.5	0.4	0.7
					Moderate / High AMD	0.6	0.5	0.8
Normalized Generality	Intercept	0.22	0.20	0.25	Reference / Moderate AMD	0.79	0.72	0.87
	Slope	1.09	1.05	1.13	Reference / High AMD	0.44	0.31	0.62
					Moderate / High AMD	0.55	0.31	0.71
Normalized Vulnerability	Intercept	0.18	0.16	0.21	Reference / Moderate AMD	0.69	0.62	0.77
	Slope	1.14	1.1	1.19	Reference / High AMD	0.27	0.18	0.40
					Moderate / High AMD	0.39	0.30	0.52

Table 2. Parameter estimates and 95% credible intervals for the effects of the AMD mining gradient on the stability metric *s*, when interaction strengths are estimated in one of four ways. The shape parameter is excluded from this summary. Derived quantities were calculated from the posterior distributions of each model. AMD impacts start at ~ -0.8 on PC axis 1, and maximum impacts are represented by values of ~-6 on PC axis 1.

Model					Relative Change			
Interaction Strength Estimate	Parameter	Median	2.5%	97.5%	Derived quantity	Median	2.5%	97.5%
Random	Intercept	0.03	0.02	0.05	Reference / Moderate AMD	2.1	1.4	3.3
	Slope	0.8	0.7	0.9	Reference / High AMD	14.2	3.0	64.1
					Moderate / High AMD	6.7	2.2	19.6
Scaled	Intercept	0.01	0.01	0.02	Reference / Moderate AMD	2.0	1.3	2.9
	Slope	0.8	0.7	0.9	Reference / High AMD	11.8	2.8	43.2
					Moderate / High AMD	5.8	2.1	14.8
Correlated	Intercept	0.04	0.03	0.07	Reference / Moderate AMD	2.0	1.3	3.2
	Slope	0.8	0.7	0.9	Reference / High AMD	12.0	2.3	59.4
					Moderate / High AMD	5.9	1.8	18.6
Scaled + Correlated	Intercept	0.03	0.02	0.05	Reference / Moderate AMD	2.0	1.3	3.1
	Slope	0.8	0.7	0.9	Reference / High AMD	11.3	2.7	52.8
					Moderate / High AMD	5.7	2.0	17.1

Figure Captions

Figure 1. Conceptual figure of the food web inference process. The probability of pairwise interactions based on Niche processes (e.g., function of predator:prey body size) are inferred (A). Neutral probability matrices (B) are calculated as the pairwise product of species relative abundances (rescaled from 0.5 to 1). These are multiplied together to calculate the interaction probability matrices (C). The probability values in this matrix are rescaled from 0 to 1 (D) and multiple Bernoulli trials are conducted based on these probabilities to create binary adjacency matrices (E). Adjacency matrices are used to calculate distributions of food web measures and estimate stability. Red, yellow and blue in matrices A-D indicate low, medium and high probability of interactions, respectively. Blue and white in adjacency matrices (E) indicate the presence and absence of inferred links, respectively.

Figure 2. Species Richness and inferred food web measures across the AMD gradient A) Species Richness; B) Links; C) Connectance; D) Normalized Generality; E) Normalized Vulnerability. AMD stress increases left to right. Points in Panel A are the total taxonomic richness for each site. Points in Panels B-D are individual values for each food web iteration and are jittered with an alpha value of 0.2 for visualization. Points are color-coded based on site. AMD impacts start at ~ -0.8 on PC axis 1, and maximum impacts are represented by values of ~-6 on PC axis 1. Blue lines are the median fitted-values and grey shading is 95% credible intervals.

Figure 3. Inferred stability metric, *s*, across the AMD gradient when varying the estimate of interaction strengths (see methods). A) Random interaction strengths; B) random interaction strengths scaled by body size; C) Random interaction strengths, positive and negative interactions correlated; D) random interaction strengths, scaled by body size, and positive and negative interactions correlated. AMD stress begins at ~-0.8, and increases left to right. Points

are individual stability values for each food web iteration and are jittered with an alpha value of 0.2 for visualization. Points are color-coded based on site. Note that in panel C and D the values of s cluster for some impacted sites (i.e. orange, yellow). Blue lines are the median fitted-values and grey shading is 95% credible intervals.

Figures

Figure 1

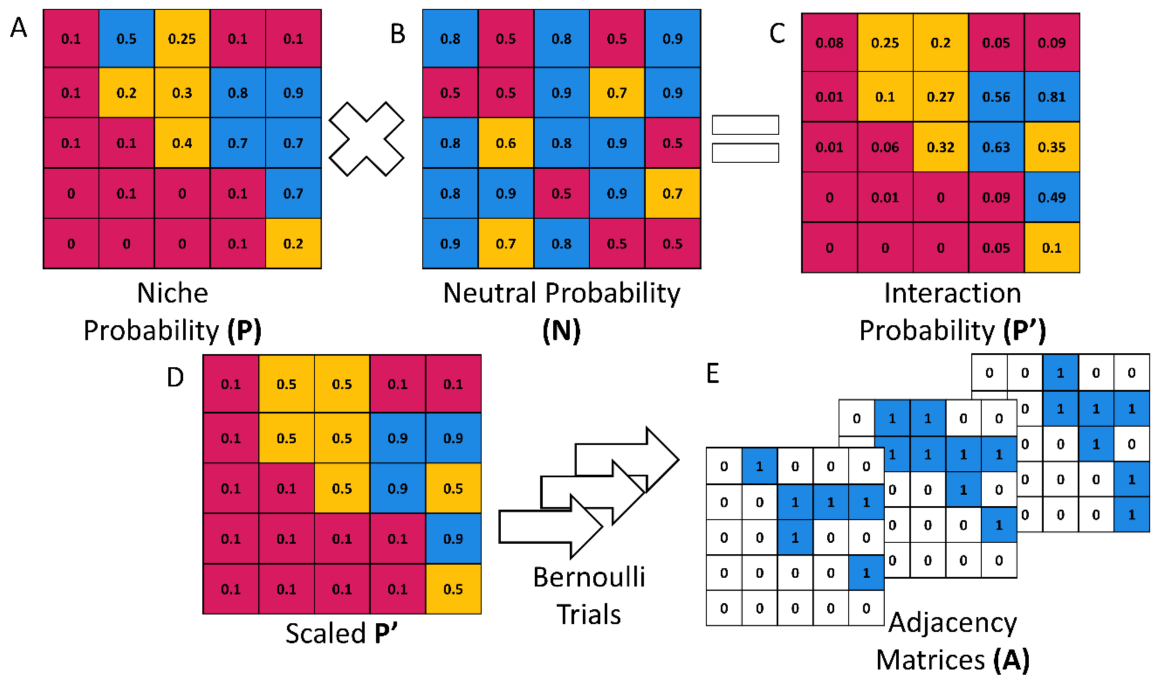

Figure 2

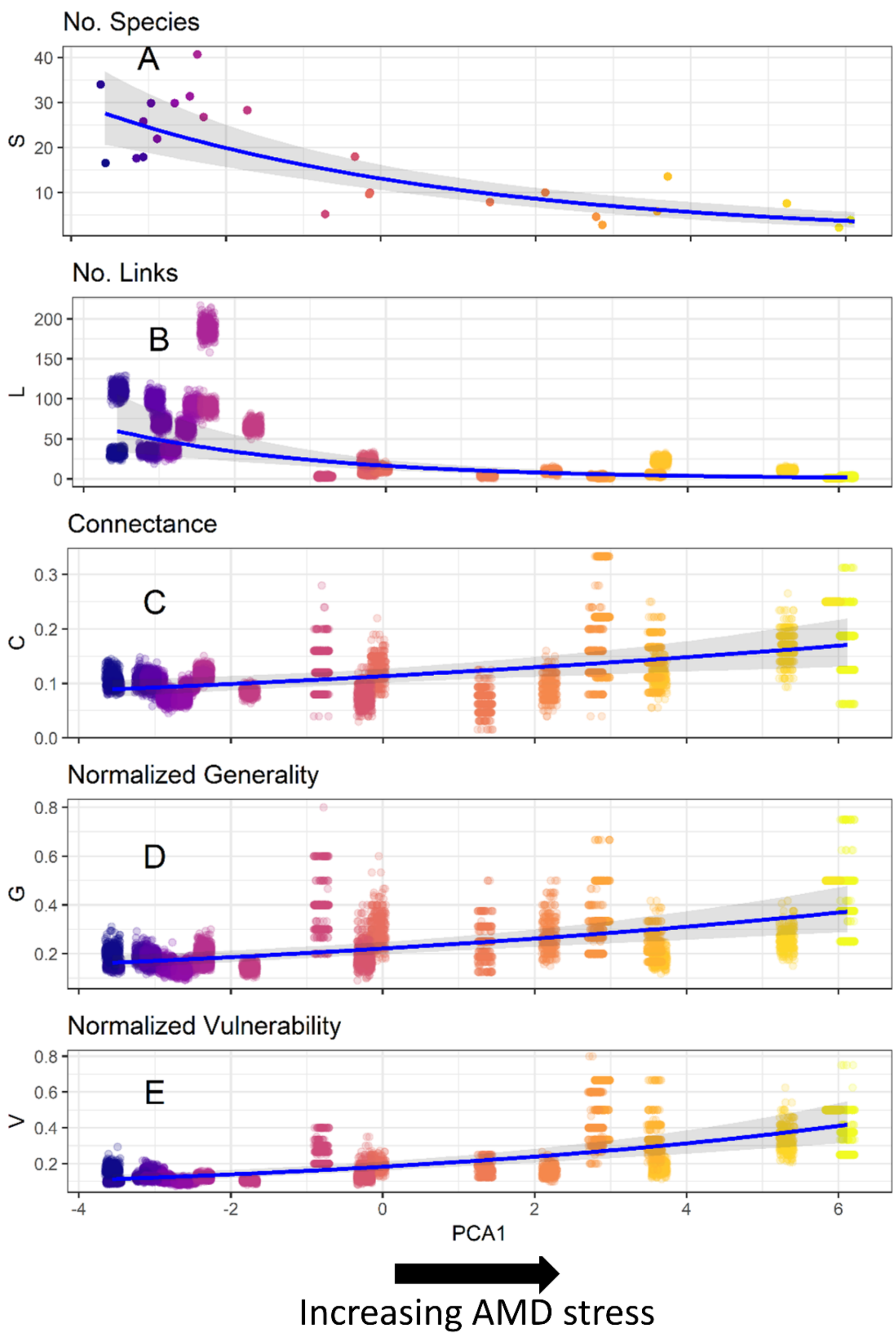

No. Species
A
S
40
30
20
10
No. Links
B
L
200
150
100
50
0
Connectance
C
C
0.3
0.2
0.1
0.0
Normalized Generality
D
G
0.8
0.6
0.4
0.2
Normalized Vulnerability
E
V
0.8
0.6
0.4
0.2
-4
-2
0
2
4
6
PCA1
Increasing AMD stress

Figure 3

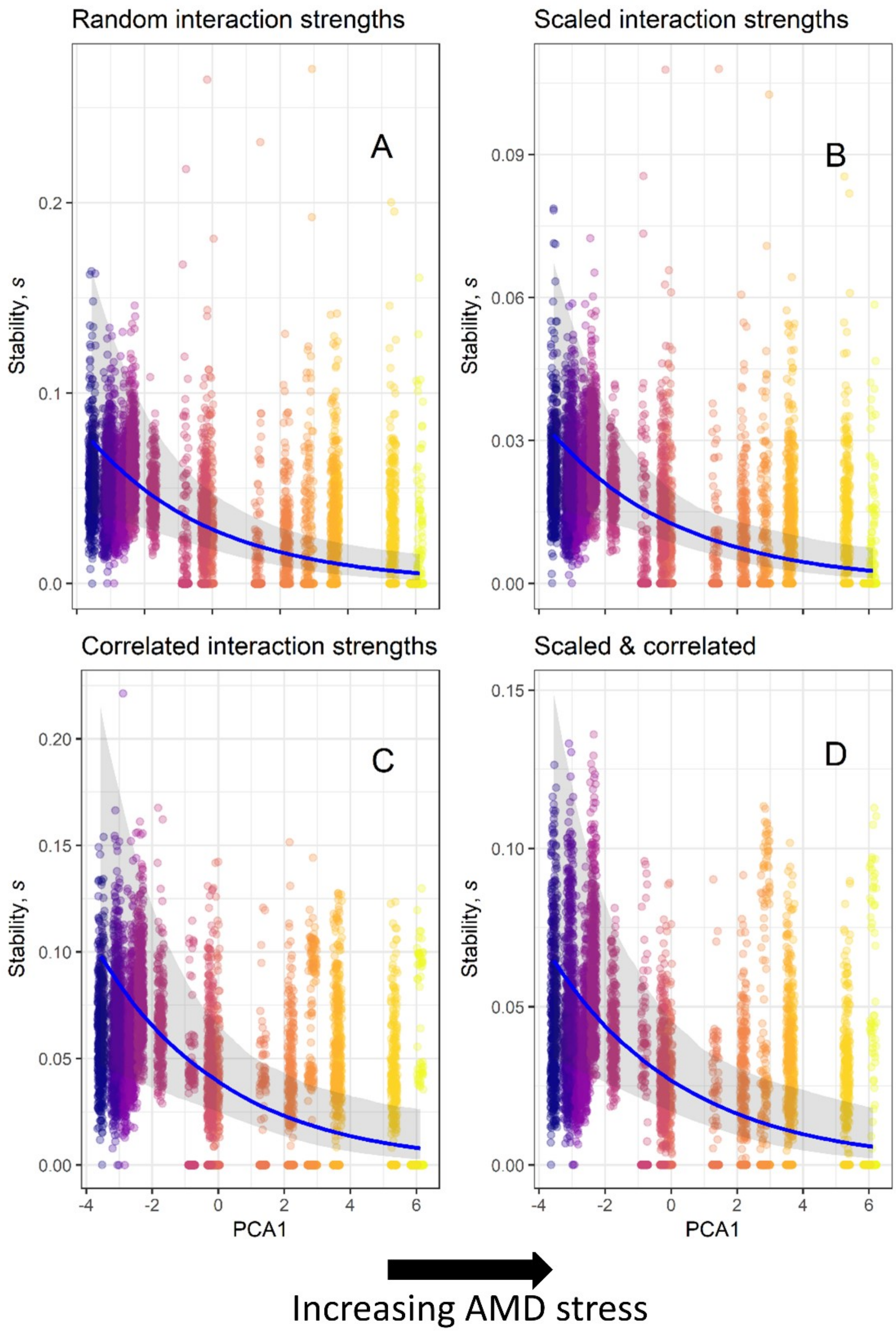

Random interaction strengths
Scaled interaction strengths
Correlated interaction strengths
Scaled & correlated
A
B
C
D
Stability, s
PCA1
0.0
0.1
0.2
0.00
0.03
0.06
0.09
0.05
0.10
0.15
0.20
-4
-2
0
2
4
6
Increasing AMD stress